Random Imperfections for Dynamic Pulse Buckling[a]

By Herbert E. Lindberg[1]

ABSTRACT: White noise and wavelength-dependent random imperfections, each represented by Fourier series having random coefficients with Gaussian distributions, are explored as representations of imperfections to be used in numerical investigations of dynamic pulse buckling. Results from a closed form solution show the relationship between these imperfections and previously used single-mode imperfections, and demonstrate the statistics of typical buckled forms. Example random imperfection shapes and growing buckle forms show the advantage of using 'gray' noise (standard deviation $\boldsymbol{\sigma}$ of the coefficients decreases as $n^{-1/2}$) rather than pure white-noise (constant $\boldsymbol{\sigma}$) imperfections. The statistics of buckle amplitudes from buckled forms with 15 or more waves are shown to give good estimates for the statistics of a large population of random buckle shapes. This is an important result for finite element calculations, in which Monte Carlo calculations would be time consuming and expensive.

INTRODUCTION

A dominant mode of response in metal cylindrical shells under impulsive pressures is dynamic pulse buckling into high order buckle modes with short wavelengths. The dominant modes typically have 20 to more than 100 waves around the circumference, depending on the material and radius-to-thickness ratio of the shell. These mode numbers must be determined as part of the solution to buckling response. In closed form analyses (Lindberg & Anderson 1968) they have been found by calculating response in a sequence of modes to find the most amplified mode. Critical impulses for threshold buckling are then estimated by representing the actual motion, which takes place in many amplified modes, by motion in only the most amplified mode (Lindberg & Florence 1987).

With this procedure it is not necessary to provide a detailed description of the imperfections that trigger buckling. It is enough to assume that random imperfections are present in all the modes, so that the buckle motion can selectively amplify the critical mode into which the shell buckles. Imperfections are then represented by an equivalent single imperfection in this mode. However, for more complex shell geometries and loadings, solutions must be found by numerical methods. In the finite element method with the shell descritized around the circumference, some other means must be used to specify imperfections so the response analysis can yield the buckle shape and critical impulse.

In this paper, it is proposed that the imperfections be taken as a nearly white noise perturbation from a perfectly circular shape. This perturbation is described by a Fourier series with random coefficients, each having a Gaussian distribution

[a]Presented at the May 20-22, 1987, ASCE Engineering Mechanics Division Specialty Conference held in Buffalo, NY.

[1]Staff Scientist & Dir., APTEK, Inc., San Jose Office, 4320 Stevens Creek Blvd., Suite 195, San Jose, CA 95129, (408) 241-7191.

in amplitude with zero mean value and standard deviation $\boldsymbol{\sigma}(n)$. The proposed form for $\boldsymbol{\sigma}$ is $\boldsymbol{\sigma} = Chn^{-1/2}$, where C is a parameter determined in the paper by comparison with experimental results and h is wall thickness. This form of departure from true white noise, in which $\boldsymbol{\sigma}$ is constant for all wave numbers, is shown to describe imperfections that are proportional to an appropriate combination of the wall thickness and the wavelength of each buckling mode.

This specification gives imperfection coefficients that decrease conservatively slowly with increasing n as compared with measurements on a limited number of shells, and is more physically reasonable than a pure white noise description, which gives a divergent series for the perturbation shape. The $n^{-1/2}$ decrease in standard deviation results in a nearly convergent series for the mean square deviation of the imperfection shape; the exponent -1/2 is the separator between convergent and divergent series.

Buckle shapes resulting from this imperfection description are calculated analytically at a sequence of increasing times. The resulting buckle shapes are compared with imperfection shapes found by truncating the imperfection series at a sequence of bandwidths ranging from a small fraction of the bandwidth of the dynamic buckling amplification function to several times this bandwidth. These examples give a physical feel for the imperfection form, the nature of its convergence, and how it is modified by pulse buckling amplification.

Buckle forms are then calculated for a large number of random imperfection shapes to determine the statistics of the amplitudes and wavelengths of the buckles. It is shown that good estimates of the statistics of the universe of buckle shapes can be obtained by calculating the statistics of the buckles in a single calculation. This is an important result for use in finite element calculations, in which Monte Carlo calculations for buckle statistics would be expensive and time consuming.

WHITE-NOISE AND SINGLE-MODE IMPERFECTIONS

Buckling from White Noise Imperfections

A mathematical analysis of random noise currents in electrical communication, described in Rice 1954, is closely analogous to the analysis of buckle shapes in long shells under radial impulse uniform around the circumference. We consider a shell with a random shape imperfection given by

$$u_i(\theta) = \sum_{n=2}^{N} [\alpha_n \cos n\theta + \beta_n \sin n\theta] \tag{1}$$

where θ is angle around the circumference, n is mode number, the coefficients α_n and β_n are random variables, each normally distributed with zero mean value and standard deviation $\boldsymbol{\sigma}$, and N is an upper limit to be determined by the buckling analysis. For clarity, we consider first that $\boldsymbol{\sigma}$ is constant for all n, just as in Rice 1954. This is called 'white noise,' by analogy to the electrical case in which u_i would be current and θ would be time. Example imperfection shapes from Eq. (1) are given in Section 3.

The resulting buckle shape is given by

$$u(\theta,\tau) = u_0(\tau) + \sum_{n=2}^{N} [a_n(\tau)\cos n\theta + b_n(\tau)\sin n\theta] \tag{2}$$

where τ is a dimensionless time. The first term is the symmetric inward motion from the symmetric impulse. The remaining terms are the growing flexural modes. The term for $n = 1$ is omitted because, to the accuracy of the buckling theory given in Lindberg & Anderson 1968 and Lindberg & Florence 1987, this term is a rigid body translation. Example buckle shapes from Eq. (2) and their growth with time are given later in the paper.

For the present, it is not necessary to be concerned with the details of any particular buckling analysis except for the fundamental result that the buckle shape coefficients $a_n(\tau)$ and $b_n(\tau)$ are expressed by the form

$$a_n(\tau) = \alpha_n G(n,\tau), \qquad\qquad b_n(\tau) = \beta_n G(n,\tau) \tag{3}$$

where $G(n,\tau)$ is an amplification function which, at times when buckle amplitudes are observable, has significant values only over a band of modes in the range $2 < n < N$. Thus, in Eqs. (1) and (2) we have used an upper limit N because higher modes have no significant growth. This is a crucial step in specifying the imperfections in Eq. (1).

The mean square of the deformed shape (averaged over θ at fixed τ) is

$$\begin{aligned} \overline{u^2}(\tau) &= \sum_{n=2}^{N} [\overline{a_n^2}(\tau)\cos^2 n\theta + \overline{b_n^2}(\tau)\sin^2 n\theta] \\ &= \boldsymbol{\sigma}^2 \sum_{n=2}^{N} G^2(n,\tau) \end{aligned} \tag{4}$$

This result follows from the independence of a_n and b_n and the identity of their distributions. From the central limit theorem for the sum of many independent random variables, the distribution of u is also random normal with zero mean. This suggests that experimental determination of the mean square of the deformed buckle shape, $\overline{u^2}(\tau)$, would give a statistical description of the deformed shape.

Note that the series in Eq. (4) converges because of the finite bandwidth of the amplified modes. A similar series for the mean square of the initial imperfection with $\boldsymbol{\sigma}$ constant for all modes (white noise) does not converge as $N \to \infty$. In the next section we suggest a physically motivated variation of $\boldsymbol{\sigma}$ with n that gives a convergent series for the imperfections themselves.

Specification of Random Imperfections

For finite element calculations, we propose that Eq. (1) be used to generate an unstressed initial deformation. The values for α_n and β_n are to be selected from a population of random numbers with zero mean value and standard deviation $\boldsymbol{\sigma}$. Then the series is summed to generate $u_i(\theta)$. Element displacements are then chosen to approximate this initial shape.

We have already mentioned that to specify random imperfections in the form given by Eq. (1) we must specify the value of N to be used in truncating the series. In a finite element analysis, this selection goes hand in hand with the selection of the element sizes such that the buckle wavelengths can be resolved. Both depend on prior knowledge of the buckle wavelengths to be expected. The calculation itself will select the buckle wavelengths that are amplified, so one could simply take N large enough and the element size small enough to allow for any possible wavelengths. However, the time and cost of the calculation increases rapidly with the number of elements, so careful choices are necessary for N and the number of elements required to resolve the corresponding wavelength. These choices can be based on the solutions in Lindberg & Florence 1987 for simple loading and geometry.

The other quantity to be specified is the magnitude of $\boldsymbol{\sigma}$. The choice of this magnitude quantity in analogous to the choices made in Lindberg & Florence 1987 for equivalent single-mode imperfections in the most amplified mode. In both cases, a reasonable approach is to base the choice on observed buckle deformations rather than on an attempt to measure the actual imperfections. These imperfections are extremely small and difficult to measure with good accuracy. Also, in practice these are 'equivalent' initial shape imperfections, that account for a range of imperfection sources, including those in wall thickness, material properties, prestresses, and so forth.

Relationship Between White-Noise and Single-Mode Imperfections

In Lindberg & Florence 1987 it was found that observed impulse thresholds for buckling in shells, over a range of radius-to-thickness ratios from 20 to 200, were reasonably well predicted by taking equivalent single-mode imperfections in the most amplified mode equal to 1% of the wall thickness. The critical impulses for buckling are relatively insensitive to the exact value of this imperfection because of the exponential growth of the buckles with increasing impulse.

The value to be used for $\boldsymbol{\sigma}$ in Eq. (1) can be made to correspond to this single-mode imperfection by means of the statistical analysis in Rice 1954. Thus, for imperfections concentrated in a single mode we have

$$u_i(\theta) = \delta_n \sin n\theta \tag{5}$$

The buckle deformation is then simply

$$u(\theta, \tau) = \delta_n G_{\max}(\tau) \sin n\theta \tag{6}$$

in which $G_{\max}$ is the maximum amplification found as described above. The mean square of this deformation is

$$\begin{aligned} \overline{u^2}(\tau) &= \delta_n^2 G_{\max}^2(\tau) \cdot \frac{1}{2\pi} \int_0^{n\theta=2\pi} \sin^2 n\theta \; d(n\theta) \\ &= \delta_n^2 G_{\max}^2(\tau) \cdot \frac{1}{2} \end{aligned} \tag{7}$$

The choice for $\boldsymbol{\sigma}$ can now be made such that this mean square is the same as the mean square given by Eq. (4) for random imperfections, with the result

$$\boldsymbol{\sigma}^2 \sum_{n=2}^{N} G^2(n,\tau) = \frac{\delta_n^2}{2} G_{\max}^2(\tau)$$

or

$$\boldsymbol{\sigma} = \frac{\delta_n G_{\max}(\tau)}{\left[2\sum_{n=2}^{N} G^2(n,\tau)\right]^{1/2}} \tag{8}$$

The above procedure assumes that the observed buckle statistic is the root mean square of the deformation. The correspondence between theory and experiment in Lindberg & Florence 1987 was actually based on the measured threshold plastic bending or plastic flow buckle deformation at the largest peaks in response. Thus, we should base the comparison between single-mode and random imperfections on the distribution of peaks rather than on the mean square deformation.

Monte Carlo calculations later in the paper give the distribution of peak-to-peak amplitudes of buckle shapes. Based on this distribution, a peak value selected from a relatively large sample size (from 10 to 50 waves were typically observed in each experiment) would be equal to about three times the rms value of deformation. If we choose this value for comparison with the single-mode theory, then

$$u_{\max} = 3\boldsymbol{\sigma}\left[\sum_{n=2}^{N} G^2(n,\tau)\right]^{1/2} \tag{9}$$

For the single-mode imperfection, $u_{\max} = \delta_n G_{\max}$. These peak deformations are equal for

$$\boldsymbol{\sigma} = \frac{\delta_n G_{\max}(\tau)}{3\left[\sum_{n=2}^{N} G^2(n,\tau)\right]^{1/2}} \tag{10}$$

Analytical Example

To determine the relationship between $\boldsymbol{\sigma}$ and δ_n according to Eq. (8) or (10), we must now specify the amplification function $G(n,\tau)$. Results given in Lindberg & Florence 1987 demonstrate that the shape of this amplification as a function of mode number is very nearly the same for both elastic and plastic-flow buckling over a wide range of shell radius-to-thickness ratios. For our purpose here, we use the equations from plastic-flow buckling in relatively thick-walled shells, for which the amplification function is given by a simple analytic expression.

The equations of motion for this case, following an initial radial impulse uniform around the shell, were derived by Abrahamson and Goodier 1962 and also in Lindberg & Florence 1987, with the result

$$u'''' + (1+s^2)u'' + s^2 u + \ddot{u} = -s(a/h + u_i + u_i'') \tag{11}$$

where

$$u = \frac{w}{h}, \qquad u_i = \frac{w_i}{h}, \qquad \hat{\tau} = \frac{c_p \alpha t}{a} \tag{12}$$

$$c_p = \sqrt{\frac{E_t}{\rho}}, \qquad s^2 = \frac{\sigma_y}{E_t \alpha^2} \qquad \alpha^2 = \frac{h^2}{12a^2} \tag{13}$$

in which $w(\theta, t)$ is radial deformation, positive inward, $w_i(\theta)$ is an initial unstressed imperfection shape, t is time, $\hat{\tau}$ is a dimensionless time, c_p is plastic wave speed, E_t is the material tangent modulus, assumed for now to be constant beyond yield, ρ is density, σ_y is yield stress, h is wall thickness, and a is shell radius. Note that the dimensionless displacements u and u_i are normalized by the wall thickness rather than by the radius as in Abrahamson and Goodier 1962 and Lindberg & Florence 1987. Primes indicate differentiation with respect to θ and dots with respect to $\hat{\tau}$.

Substitution of the series expansions

$$u_i(\theta) = \sum_{n=2}^{N} (\alpha_n \cos n\theta + \beta_n \sin n\theta) \tag{14}$$

$$u(\theta, \tau) = a_0(\tau) + \sum_{n=2}^{N} [a_n(\hat{\tau}) \cos n\theta + b_n(\hat{\tau}) \sin n\theta] \tag{15}$$

into equation of motion (11) gives

$$\ddot{a}_0 + s^2 \left(\frac{a}{h} + a_0 \right) = 0 \tag{16}$$

$$\ddot{a}_n + [n^4 - n^2(1 + s^2) + s^2] a_n = s^2 (n^2 - 1) \alpha_n \tag{17}$$

A similar equation results for b_n. Pulse buckling modes have $n^2 \gg 1$, so Eq. (17) can be simplified to

$$\ddot{a}_n + s^2 \eta^2 (\eta^2 - 1) a_n = s^4 \eta^2 \alpha_n \tag{18}$$

where $\eta = n/s$.

The solution to Eq. (18) with initial conditions $u(\theta, 0) = \dot{u}(\theta, 0) = 0$ is

$$a_n(\tau) = \frac{\alpha_n}{1 - \eta^2} \left[\begin{matrix} \cosh \\ \cos \end{matrix} \; p_n \tau \; - 1 \right] \tag{19}$$

in which we have introduced a new dimensionless time τ and an argument parameter p_n defined by

$$\tau = s^2 \hat{\tau}, \qquad p_n = \eta |1 - \eta^2|^{1/2} \tag{20}$$

The cosh functions are taken for $\eta < 1$ and the cos functions for $\eta > 1$.

The function multiplying α_n in Eq. (19) is called the amplification function. Fig. 1 gives an example of this function plotted against mode number n for $\tau = 6$ and mode number parameter $s = 20.67$. This value results for an aluminum 6061-T6 ($\sigma_y / E_t = 0.5$) shell with radius-to-thickness ratio 8.4. This is a thicker shell than normally of interest, but the value of s is convenient for numerical results given later in the paper.

An important feature of the amplification function is that at values of τ large enough for significant amplification, a band of modes are amplified with mode numbers ranging from somewhat below to somewhat above the value s. Neither very low nor very high order modes are amplified significantly. Also, the shape

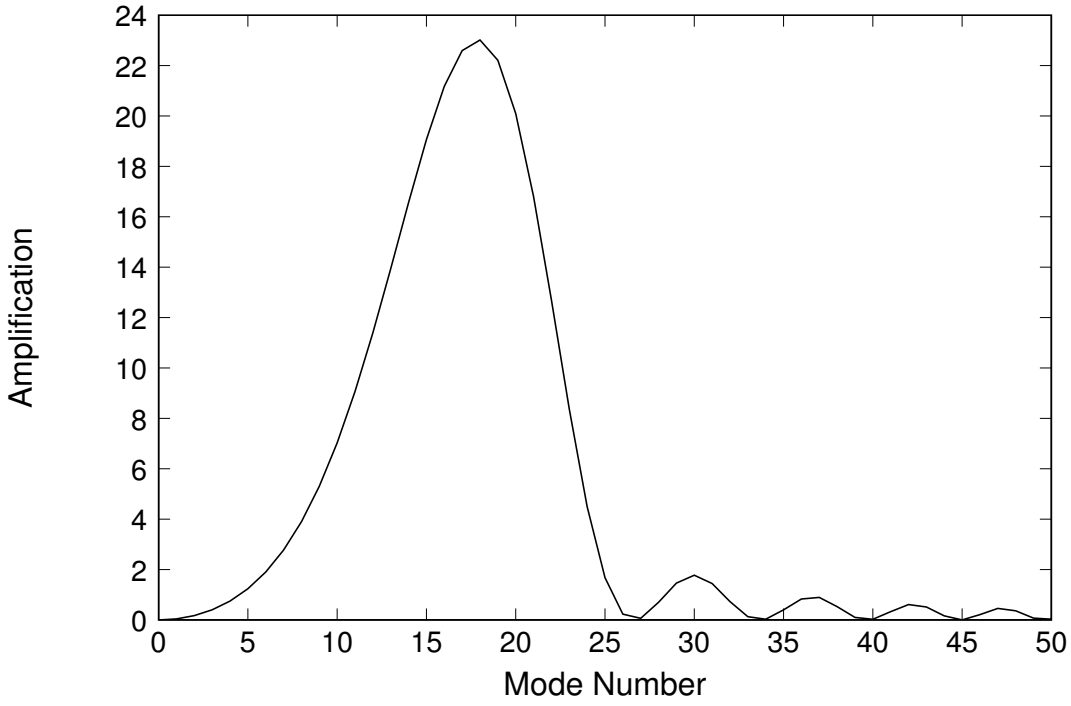

Figure 1: Amplification Function from Equation (19) for $\tau = 6$.

of the amplification function is independent of s, as can be seen from Eq. (19); amplification depends only on η and τ. Furthermore, even in thinner shells, which buckle during elastic or elastic-plastic radial motion, and for which the amplification function must be found by numerical integration, the resulting amplification function when plotted against a normalized wave number has essentially the same shape as that of the analytical result here.

These two properties of the amplification function have important implications for the results in this paper. The finite lower and upper mode number bounds and the universal shape, taken together, allow a convenient definition (in Section 3) of random imperfections that are proportional to an appropriate combination of wall thickness and buckle wavelengths. The universal shape allows Monte Carlo calculation of buckle waveform statistics that can be applied quite generally.

The relationship between white noise and equivalent single-mode imperfections can now be calculated quite generally from Eqs. (10) and (19). With $G(\eta, \tau)$ from Eq. (19), the G terms in Eq. (10) can be expressed as

$$\frac{1}{G_{\max}(\tau)} \left[\sum_{n=2}^{N} G^2(\eta, \tau) \right]^{1/2} = s^{1/2} R(\tau) \tag{21}$$

where

$$R(\tau) = \frac{1}{G_{\max}(\tau)} \left[\int_{\eta_1}^{\eta_2} \frac{1}{1-\eta^2} \left(\begin{matrix} \cosh \\ \cos \end{matrix} \; p(\eta, \tau) \; - \; 1 \right) d\eta \right]^{1/2} \tag{22}$$

in which we have used $d\eta = \Delta n / s = 1/s$ so that the sum can be replaced by an integral (s is typically large enough that η can be treated as a continuous variable). Numerical integration of Eq. (22) shows that $R(\tau)$ depends weakly on τ. In the range $5 < \tau < 11$, $R(\tau)$ varies from 0.640 to 0.521. Since in this range $G_{\max}$

varies from 14 to 272, thresholds for buckling will certainly occur in this range. We therefore take $R = 0.60$ and the relationship between single-mode and random imperfections in Eq. (10) becomes

$$\boldsymbol{\sigma} = \frac{\delta_n}{3s^{1/2}R(\tau)} = 0.556\ \delta_n s^{-1/2} \tag{23}$$

Thus, the standard deviation of white noise imperfections to be used in finite element calculations decreases as $s^{-1/2}$ and hence as the inverse square root of the number of modes in the amplified range. This result occurs because we are adding each mode as a random variable and the deviation of the sum increases in a root-mean-square fashion. If we are to relate this deviation to experimental results based on equivalent single-mode imperfections, as indicated in Eq. (23), we must therefore know the bandwidth of the modes of buckling, which is part of the solution.

This bandwidth can be estimated on the basis of the same analytical solution used to obtain $G(\eta, \tau)$ in the above discussion. From the results given in Lindberg & Florence 1987, pages 145 to 149, for representative aerospace metals at thresholds of pulse buckling, the material property parameter in the definition of s in Eqs. (13) is given by

$$\frac{\sigma}{E_t} = \left(\frac{8K}{3}\right)^{1/2} \frac{h}{a} \tag{24}$$

In this more general theory, instantaneous stress σ rather than yield stress σ_y is used, and both σ and E_t are assumed to vary with compressive strain according to a stress-stain relationship characterized by the yield strain and a shape factor K. The right hand side of Eq. (24) gives the value of the material property ratio at the final compressive hoop strain imparted by the critical impulse for buckling, which depends on the radius-to-thickness ratio of the shell as given in the formula. Substitution of Eq. (24) into Eq. (13) gives

$$s^2 = 12 \left(\frac{8K}{3}\right)^{1/2} \frac{h}{a} \frac{a^2}{h^2} = (384\ K)^{1/2} \frac{a}{h} \tag{25}$$

With this value for s, Eq. (23) becomes

$$\boldsymbol{\sigma} = 0.264\ K^{1/8} \left(\frac{a}{h}\right)^{-1/4} \delta_n \tag{26}$$

In Lindberg & Florence 1987, equivalent single-mode imperfections of $\delta_n = 0.01\, h$ are shown to give reasonable agreement between experiment and theory for critical impulses at thresholds of observable buckles. The corresponding standard deviation of white noise imperfections from Eq. (26) for $K = 15$ (an appropriate value for hardened alloys of aluminum, titanium and magnesium) and $a/h = 100$ is $0.0012\ h$.

For finite element calculations, the magnitude of imperfections to correlate theory and experiment are expected to be larger than this value because of neglect in the analytical theory of the decrease in hoop thrust with increasing buckle growth. Thus, near and beyond the threshold of significant buckling, in the analytical theory the buckle amplitudes grow unrealistically with increasing time and hence increasing impulse.

RANDOM IMPERFECTIONS PROPORTIONAL TO WALL THICKNESS AND BUCKLE WAVELENGTHS

The white noise imperfections discussed in the previous section are physically unsatisfying because the resulting Fourier series for the imperfections does not converge. It was nevertheless possible to use this form because the finite bandwidth of the series for the buckle shapes gave truncated and hence bounded series for buckle shapes. However, this puts a premium on specification of the bounding mode number N to be used in calculating response with finite element methods. If N is made conservatively large, the imperfections have large amplitude components at short wavelengths that may be difficult to treat numerically even though they are eventually suppressed in comparison with the dominant shape of the buckled form, which grows with time.

It is therefore useful to explore other forms of random imperfections that are better behaved and are based on expectations for imperfections to be found in actual shells. One such form is explored in this section. Other forms may be appropriate for specific applications in which information is available about the manufacturing processes that introduce imperfections.

In the remainder of this section we first give example imperfection shapes to demonstrate the difficulty with white noise imperfections discussed above. Then we describe the proposed alternative form of random imperfections and show how this form relates to single-mode imperfections. Example imperfection shapes with this form are compared with the white noise shapes for the same set of random numbers. Then the buckle shapes that result from these imperfections are given at a sequence of increasing times, to show how the buckling process greatly modifies the imperfection shape and increases its amplitude.

White Noise Imperfection Shapes

Fig. 2 gives imperfection shapes calculated with Eq. (1) for random coefficients α_n and β_n having a Gaussian distribution and a constant standard deviation of unity. In the left graph the series is truncated at $N = 20$ and in the right graph at $N = 50$.

If we assume that buckling is to be investigated for a problem having the amplification function in Fig. 1, then the mode numbers of most concern range from about 10 to 25, with the most amplified modes having numbers near 20. However, in a finite element calculation we have little apriori knowledge of this function except that its general shape will be similar to that in Fig. 1. We would therefore have to take N conservatively large to ensure that the significantly amplified components are included in the calculation.

Without extensive experience, it is unlikely that one would know the dominant wavelengths to within a factor of two, so even a value of $N = 50$ would not be too conservative in a calculation for which the amplification function turns out to have the amplified band given in Fig. 1. Comparison of the white noise imperfection shapes in Fig. 2 for $N = 20$ and $N = 50$ shows a substantial difference in both shape and amplitude. With $N = 20$, the peaks have amplitudes less than 10, while with $N = 50$ peaks have amplitudes greater than 20. Also, the wavelengths

associated with these peaks are about a factor of 2.5 shorter than with $N = 20$.

Thus, while the buckle motion will not amplify these short wavelengths, they tend to dominate the imperfection shape and hence require accuracy in the calculation at these wavelengths. The imperfection form described in the following paragraphs relieves this accuracy requirement while better representing physically expected forms of imperfections.

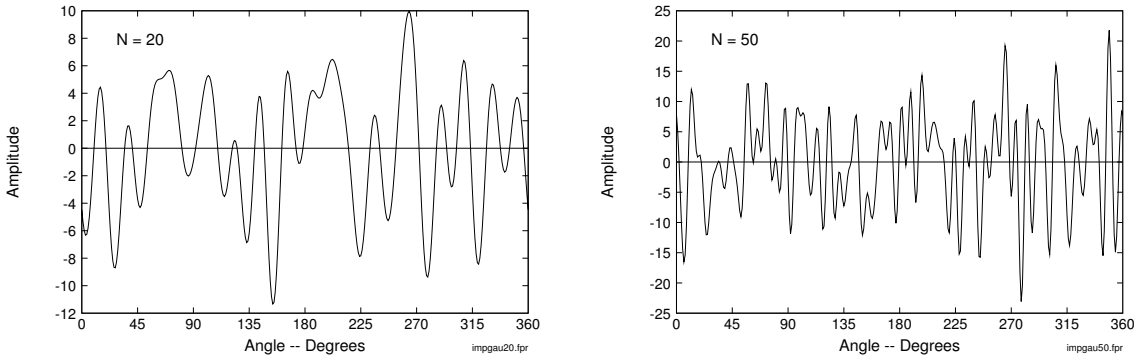

Figure 2: White noise imperfections truncated at $N = 20$ (left plot) and $N = 50$ (right plot).

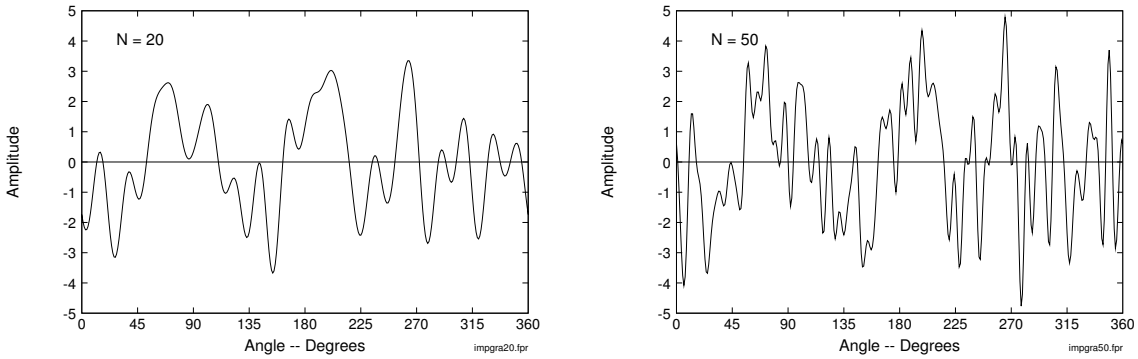

Figure 3: Gray noise imperfections truncated at $N = 20$ (left plot) and $N = 50$ (left plot). [The rationale for gray noise is given in next section.]

Adaptation of Imperfection Formula from Static Buckling

Near the turn of the century, hundreds of experiments were performed on static axial buckling of columns to determine values of imperfections to be used in design (Marston 1898, Lilly 1913 & Salmon 1921). The approach in those experiments was the same as that used in Lindberg & Florence 1987 for dynamic pulse buckling, namely that, because the imperfections were too small and diverse to measure, equivalent imperfections were calculated on the basis of observed buckling deformations interpreted with the theory to be used in design analysis.

Although the imperfections scattered widely, the general trend suggested use of the following formula in column design:

$$a_1 = 0.1\,\frac{r^2}{c} + \frac{L}{250} = \frac{1}{60}\left(h + \frac{L}{12.5}\right) \tag{27}$$

in which a_1 is the coefficient of an equivalent imperfection in the half sinewave shape $\sin \pi x/L$ of the Euler column of length L, r is the radius of gyration of the cross section and c is the distance from the neutral axis to an extreme fiber. This is Eq. (2.2.24) from Lindberg & Florence 1987. In the second expression the formula is applied for the specific case of a rectangular column of depth h.

The essential observation used in suggesting Eq. (27) was that column imperfections are expected to have two components, one proportional to its depth and the other proportional to its length. It is reasonable to take a similar approach for pulse buckling of shells. In this case, the length is the half wavelength of each buckling mode. We therefore take the standard deviation of the random imperfection coefficients in the form

$$\boldsymbol{\sigma} = C\left(h + \frac{L_n}{12.5}\right) = Ch\left(1 + \frac{\pi a}{12.5\, n}\right) = Ch\left(1 + \frac{a}{4hn}\right) \tag{28}$$

While this form is more physically reasonable than pure white noise, in that the coefficients become smaller at shorter wavelengths, the constant term, proportional to shell thickness, gives a component that is white noise and hence gives a Fourier series for the imperfections that does not converge. It is therefore useful to replace this expression by a function that converges while giving approximately the same values for $\boldsymbol{\sigma}$ as from Eq. (28) over the bandwidth of concern for pulse buckling.

One such function is

$$\boldsymbol{\sigma} = Bhn^{-1/2} \tag{29}$$

This is a convenient form that matches the values from Eq. (28) to within 20% and more frequently within 10% for all shells of interest. A good match is obtained because the exponent $-1/2$ is midway between the exponents 0 and -1 in Eq. (28). Also, this exponent is the separator between imperfections series that do and do not converge; an expression analogous to Eq. (4) shows that the terms for the variance of the imperfection shape decrease as $1/n$, which is the harmonic series.

An exact match between Eqs. (28) and (29) is forced at the peak of the amplification function, which gives

$$B = Cn_{cr}^{1/2}\left(1 + \frac{a}{4hn_{cr}}\right) \tag{30}$$

where n_{cr} is the mode number of the most amplified mode, which from Eq. (25) is given by

$$n_{cr} = \frac{s}{\sqrt{2}} = (96\,K)^{1/4}\left(\frac{a}{h}\right)^{1/2} \approx 6\left(\frac{a}{h}\right)^{1/2} \tag{31}$$

In the last expression we have taken $K = 15$, for which $(96\,K)^{1/4} = 6.16$.

With this value for n_{cr}, substitution of Eq. (30) into Eq. (29) yields the desired expression for imperfection deviations:

$$\boldsymbol{\sigma} = C\sqrt{6}\left(\frac{a}{h}\right)^{1/4}\left[1 + \frac{1}{24}\left(\frac{a}{h}\right)^{1/2}\right] hn^{-1/2} \tag{32}$$

Over the bandwith of significantly amplified modes, from $0.5\,n_{cr}$ to $1.5\,n_{cr}$, see Fig. 1, deviations from Eq. (32) match those from Eq. (28) to within 10% for $a/h > 100$. The match improves with increasing a/h. At $a/h = 10$, the thickest

shell of interest, the match is within 20%. These accuracies are far better than our knowledge of imperfection amplidudes, so Eqs. (28) and (32) are essentially equivalent.

Relationship with Single-Mode Imperfections

With $\boldsymbol{\sigma}$ now varying with n as given by Eq. (32), Eq. (4) for $\overline{u^2}(\tau)$ becomes

$$\overline{u^2}(\tau) = A^2 \sum_{n=2}^{N} \frac{1}{n} G^2(n,\tau) \tag{33}$$

where

$$A = C\sqrt{6} \left(\frac{a}{h}\right)^{1/4} \left[1 + \frac{1}{24}\left(\frac{a}{h}\right)^{1/2}\right] h \tag{34}$$

Substitution of $n = \eta s$ and $d\eta = 1/s$ into Eq. (33) gives

$$\overline{u^2}(\tau) = A^2 \int_{\eta_1}^{\eta_2} \eta^{-1} G^2(\eta,\tau)\, d\eta \tag{35}$$

If we relate single-mode and random imperfections by setting three times the root-mean-square buckle deformation equal to the peak deformation with a single-mode imperfection, as was done for Eq. (10), we obtain

$$3A \left[\int_{\eta_1}^{\eta_2} \eta^{-1} G^2(\eta,\tau)\, d\eta\right] = \delta_n G_{\max} \tag{36}$$

from which

$$A = \frac{\delta_n}{3} \cdot \frac{1}{R_1(\tau)} \tag{37}$$

where

$$R_1(\tau) = \frac{1}{G_{\max}(\tau)} \left[\int_{\eta_1}^{\eta_2} \eta^{-1} G^2(\eta,\tau)\, d\eta\right]^{1/2} \tag{38}$$

Integration to find $R_1(\tau)$ gave values from 0.705 to 0.605 for τ in the range of interest from 5 to 11. The small change in R_1 reflects the nearly constant shape of the amplification function in this range. If we take $R_1 = 0.65$, then

$$A = \frac{\delta_n}{3(0.65)} = 0.51\,\delta_n \tag{39}$$

The expression depending on a/h in the definition of A in Eq. (34) evaluates to values from 2.51 to 4.48 for a/h in the range 20 to 100 where most of the experiments reported in Lindberg & Florence 1987 were performed. We take a value of 3 to solve for C from Eqs. (34) and (39), which gives

$$C\sqrt{6} = \frac{0.51\,\delta_n}{3h} = 0.17\,\frac{\delta_n}{h} \tag{40}$$

Assuming $\delta_n = 0.01\,h$, as was done for white noise imperfections, substitution of Eq. (40) into Eq. (32) results in the following expression for the standard deviations of random imperfections:

$$\boldsymbol{\sigma} = 0.0017 \left(\frac{a}{h}\right)^{1/4} \left[1 + \frac{1}{24}\left(\frac{a}{h}\right)^{1/2}\right] h n^{-1/2} \tag{41}$$

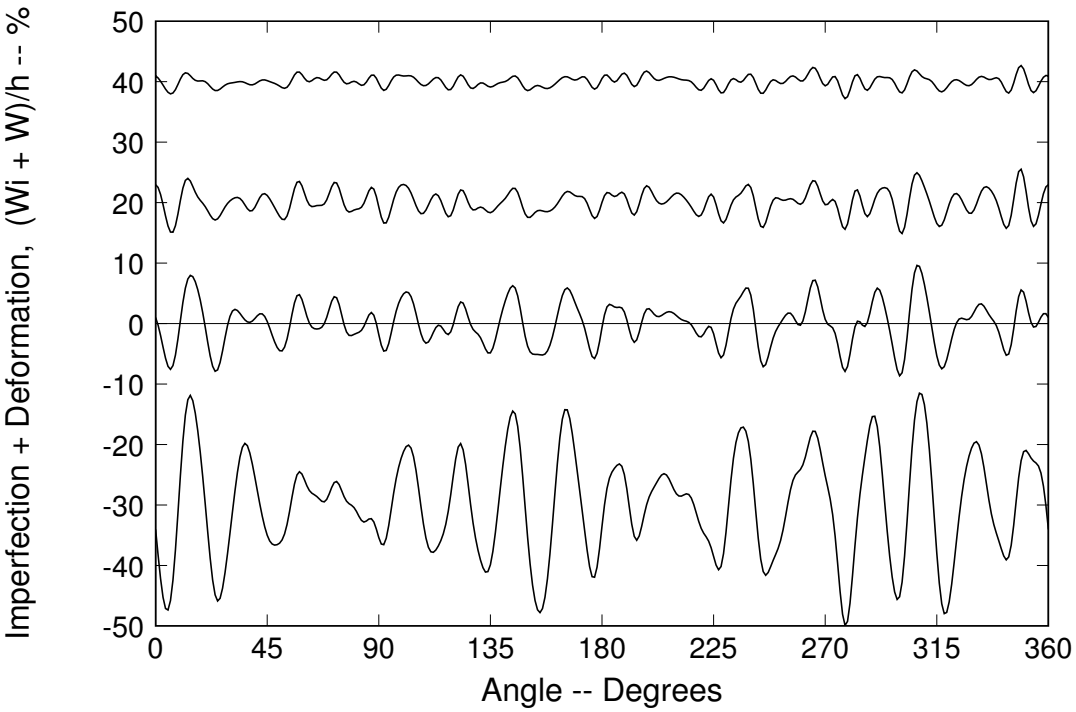

Figure 4: Buckling with white noise truncated at $N = 50$, buckle parameter $s = 20.7$, $\tau = 0$, 2, 4, 6.

When used in the analytical theory in Lindberg & Florence 1987, these deviation magnitudes will result in random buckle shapes comparable in magnitude to those for single-mode imperfections. However, as pointed out previously, the magnitude of imperfections to be used in finite element calculations are probably larger than these from the analytical theory because of neglect in the analytical theory of hoop thrust reduction as the buckles grow.

Example Imperfection and Buckle Shapes

The improved behavior of random imperfection shapes with Fourier coefficients proportional to $n^{-1/2}$ is demonstrated in Fig. 3. These were calculated with Eq. (1) using coefficients from Eq. (29) with $Bh = 1$ and the same set of 100 random coefficients used to calculate the truncated white noise imperfection shapes given in Fig. 2. The truncation numbers N are also the same in both pairs of graphs, so the sets can be compared graph by graph.

For both white and gray noise, amplitudes are higher for $N = 50$ than for $N = 20$. However, for white noise coefficients the shape with $N = 50$ is dominated by short wavelengths while for gray noise coefficients the amplitudes of the longer wavelengths remain dominant with $N = 50$. Thus, in Fig. 3 the longer wavelength features with $N = 20$ are still apparent with $N = 50$. In a similar comparison in Fig. 2 for white noise, the long wavelength features of the imperfection shape with $N = 20$ are barely detectable in the shape with $N = 50$. Other comparisons can be made for other trunctation modes with the same result.

It is also instructive to observe how the initial imperfection shape transforms into a buckled shape under the influence of pulse buckling amplification. Fig. 4

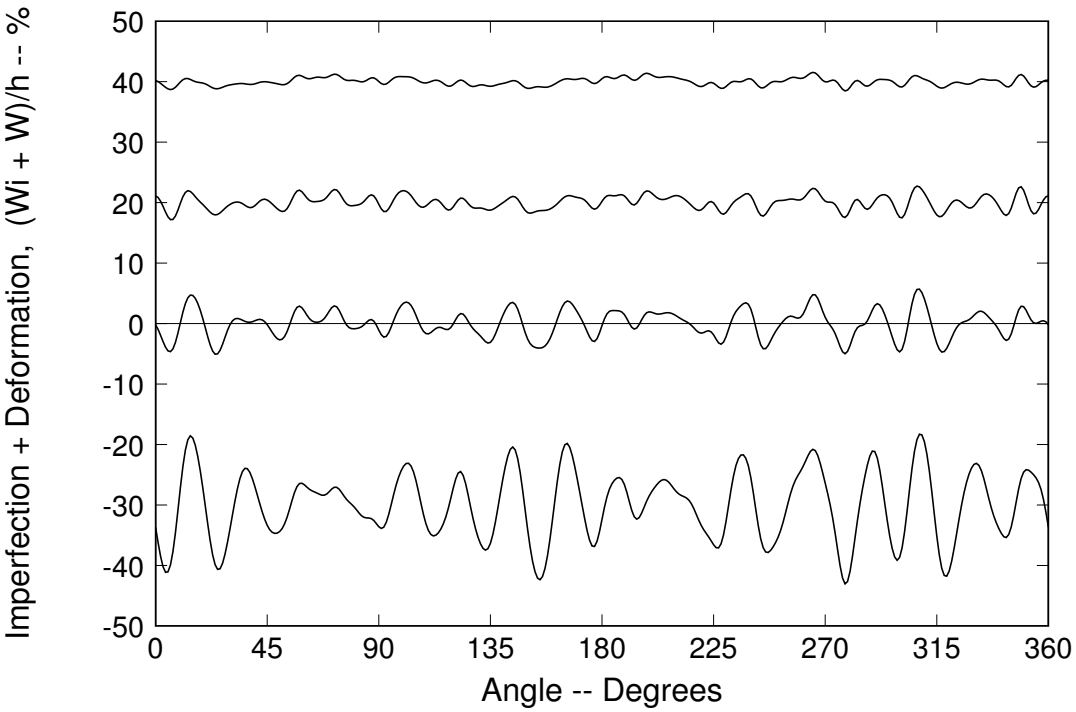

Figure 5: Buckling with gray noise truncated at $N = 50$, buckle parameter $s = 20.7$, $\tau = 0$, 2, 4, 6.

gives a series of snapshots of buckle shapes at dimensionless times $\tau = 0$, 2, 4 and 6. These were calculated with the imperfection shape in Fig. 2 with $N = 50$ using the amplification function from Eq. (19) with $s = 20.7$ (the function at $\tau = 6$ is given in Fig. 1). The baseline is shifted in the plots for $\tau = 0$, 2 and 6 to allow all four plots to be placed in the figure. The imperfection shape, at $\tau = 0$, is the same as that for $N = 50$ in Fig. 2 except for the scale change and $\boldsymbol{\sigma}/h = 0.122\%$, found from Eq. (23) with $\delta_n = 0.01\,h$ and $s = 20.7$.

The quantity plotted is the 'total' buckle shape, consisting of the sum of the imperfection and the buckle deformation. This is done to illustrate that by $\tau = 6$ there is little evidence of the imperfection shape in the total buckle shape even though the maximum peak has increased by only a factor of 7. The short wavelength features essentially disappear with increasing time. At $\tau = 2$ and 4, there is much short wavelength activity. By $\tau = 6$ this activity has ceased and a dominant buckle form has been established.

Fig. 5 gives a similar plot for growth of the gray noise imperfections in Fig. 3 but with $\boldsymbol{\sigma} = 0.32\,n^{-1/2}$, found from Eq. (41) with $a/h = 8$. The buckle shape at $\tau = 6$ is virtually identical with that in Fig. 4 for white noise, except that the amplitude is smaller because of the approximations made in deriving the coefficient expressions in Eqs. (23) and (41). A similar comparison at $\tau = 8$ is given in Fig. 6. The two buckle shapes are essentially the same and are very nearly the same as the shapes at $\tau = 6$. Thus, beyond $\tau = 6$ the main change with time is simply an increase in the amplitude of this established shape. This occurs even though the theory is linear. In a finite element calculation which includes plastic yielding in the form of hinges at the buckle peaks, the wavelengths also become fixed as time increases. Thus, this simple theory contains many of the features of a more

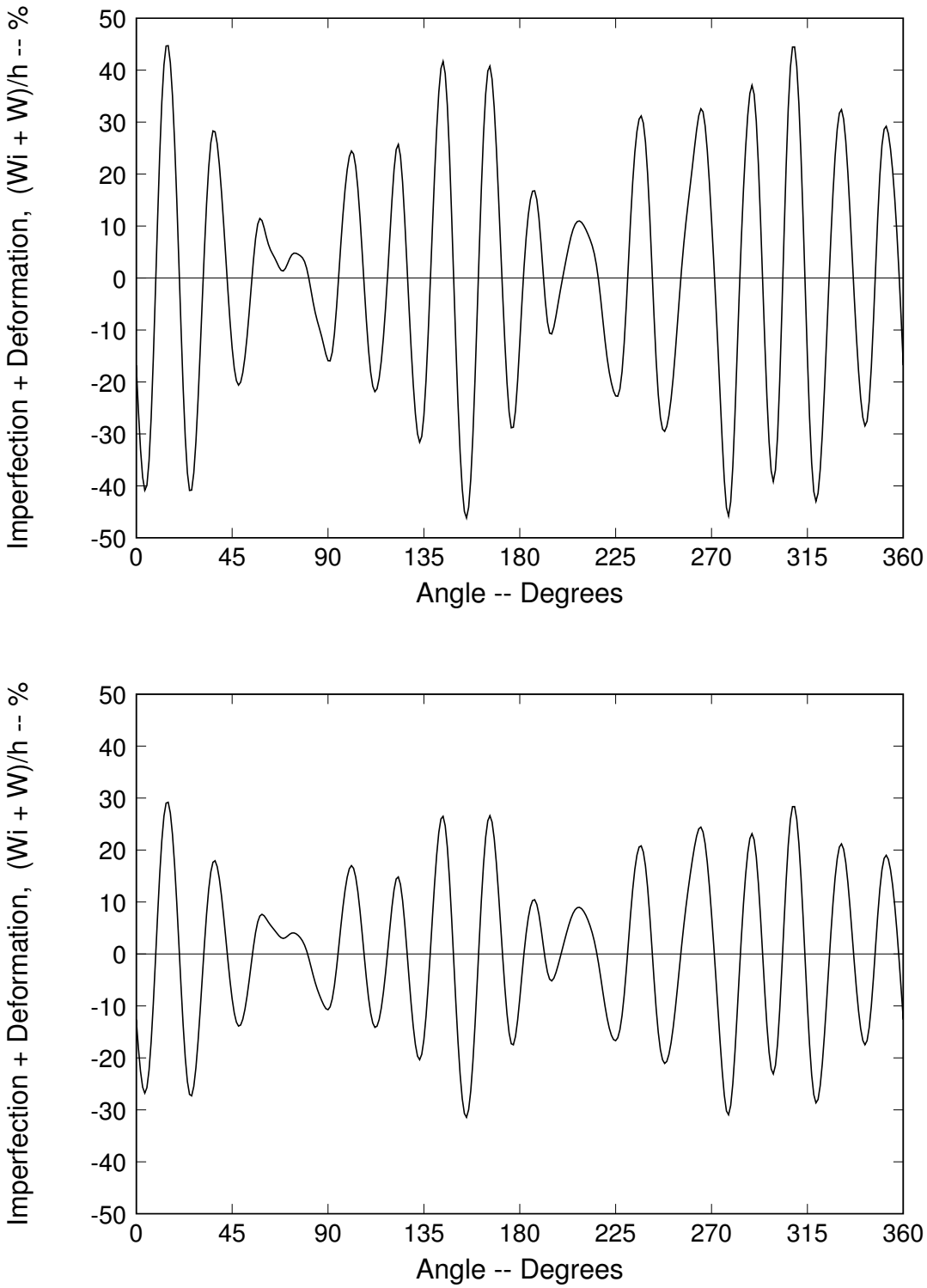

Figure 6: Buckle shapes at $\tau = 8$ for white noise (top) and gray noise (bottom) imperfections.

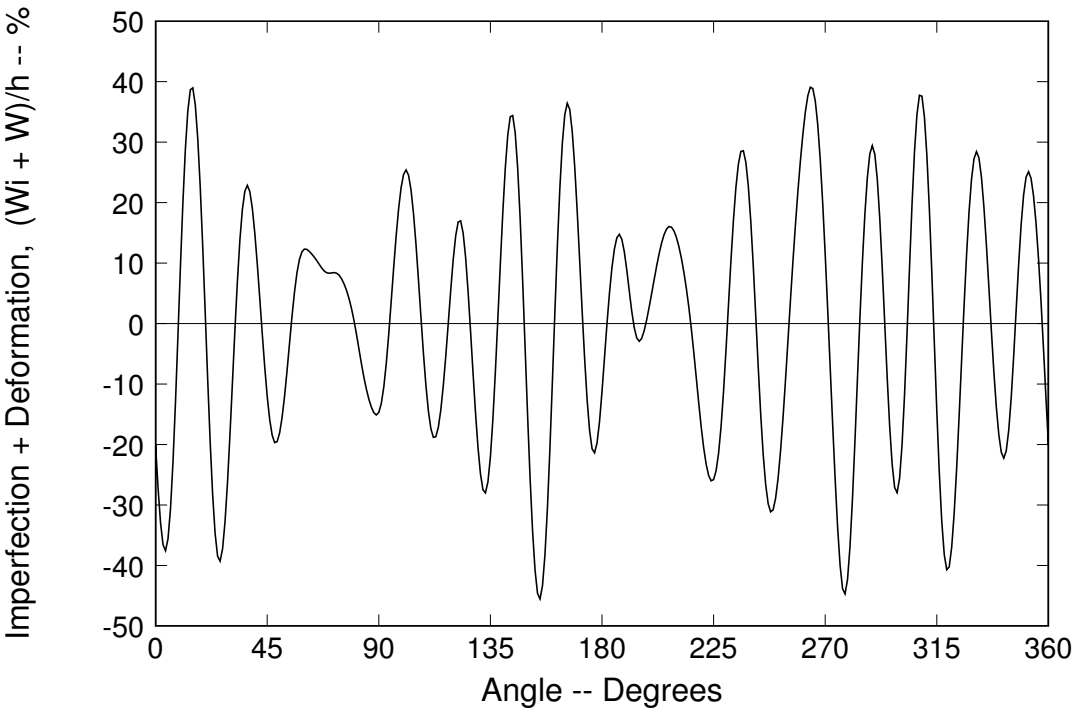

Figure 7: Buckle shape at $\tau = 8$ for "black" noise, in which $\boldsymbol{\sigma}/h = 1.75/n\%$, again with the same set of 100 random coefficients as in the previous figures.

complete analysis.

Fig. 7 gives the buckle shape at $\tau = 8$ for 'black' noise, in which $\boldsymbol{\sigma}/h = 1.75/n\%$, again with the same set of 100 random coefficients as in the previous figures. With this more rapidly decreasing standard deviation, the Fourier series for the imperfection shape converges; contributions from very short wavelength terms become negligible (black) with increasing n. Measurements by Kirkpatrick (personal communication from S. W. Kirkpatrick, SRI International, Menlo Park, California) of imperfections in aluminum shells made by rolling and welding sheet stock gave high order harmonic amplitudes that decreased at about this rate. The coefficient 1.75 was selected so that the amplitude of the buckles are about the same as for the white noise result in Fig. 6. There are some differences between the buckles from white and black noise, but the overall buckle pattern, particularly of the larger peaks, is very nearly the same for these extreme cases of noise amplitude attenuation with increasing n.

Thus, the exact nature of the attenuation is unimportant in an analytic theory in which any desired spatial resolution is obtained by simply including more terms in the solution. The importance of the attenuation is in describing imperfections for finite element analysis with a limited number of elements. Gray noise is suggested for such use because it gives conservatively large coefficients at high mode numbers while significantly reducing the amplitude of unimportant harmonics.

STATISTICS OF BUCKLE SHAPES

With imperfections in random form, the resulting buckle shapes are also random and must be described statistically. The mathematical transformation from imper-

fections to buckle shapes is too complex to allow analytical formulation of buckle statistics even for the simple buckling theory summarized in Section 2. The single exception is the mean wavelength, for which an explicit formula is given in Lindberg & Florence 1987 based on a derivation in Rice 1954. More general statistics were therefore calculated for analytical buckle shapes by the Monte Carlo method.

The same situation is true for finite element calculations except that Monte Carlo calculations would be much more time consuming and expensive. We therefore also investigated how well the statistics of buckle shapes from single buckle calculations estimate the statistics of the universe of buckle shapes. The statistics examined are the means and standard deviations of the wavelengths and peak-to-peak amplitudes of the buckle shapes.

Random Number Generator

The random number generator used for these calculations (and those in Section 3) is the function **random** in Turbo Pascal running on an IBM PC-AT. This function returns random numbers uniformly distributed in the interval 0, 1. Thus, a function x, with mean value zero and uniformly distributed in the interval $-1/2$, $1/2$ is given by

$$x = \text{random} - \frac{1}{2} \tag{42}$$

The standard deviation of x is found from

$$\boldsymbol{\sigma}_x^2 = \int_{-1/2}^{1/2} x^2 p(x)\, dx = \frac{1}{12} \tag{43}$$

where the probability density function $p(x) = 1$ for the unit interval.

From the central limit theorem, random numbers with a Gaussian distribution are obtained by adding M values of x.

$$y = \sum_{i=1}^{M} x_i = \sum_{i=1}^{M} \text{random} - \frac{M}{2} \tag{44}$$

The standard deviation of M independent random variables is

$$\boldsymbol{\sigma}_y^2 = M\boldsymbol{\sigma}_x^2 \tag{45}$$

The desired random numbers with zero mean value and unit standard deviation are therefore obtained with

$$z = \left(\sum_{i=1}^{M} \text{random} - \frac{M}{2}\right)\left(\frac{12}{M}\right)^{1/2} \tag{46}$$

The Gaussian distribution function in Eq. (46) was checked for $M = 10$ by creating a histogram from 1000 calls to the function z. The resulting histogram was a good approximation to a Gaussian distribution. All the calculations in the paper were therefore made with $M = 10$.

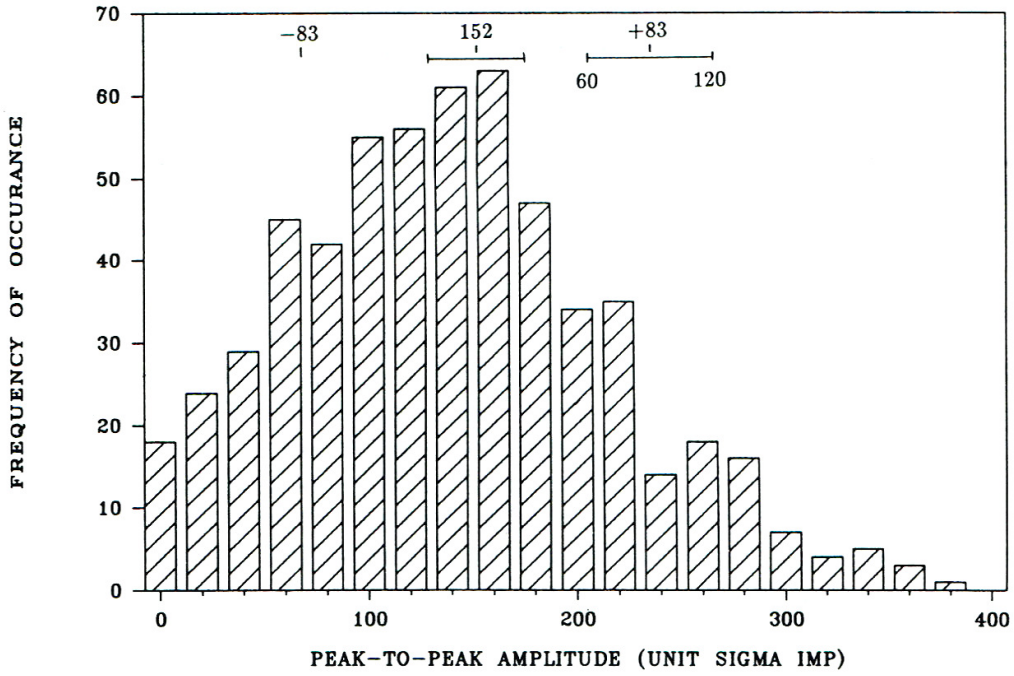

Figure 8: Histogram of buckle amplitudes for $s = 20.7$, $\tau = 6$ and unit standard deviation of imperfection coefficients.

Statistics of the Universe of Buckle Shapes

Population statistics of a universe of buckle shapes were approximated by calculating 16 buckle shapes as in the upper graph in Fig. 6 with a different set of 100 random numbers for the imperfections in each case. Imperfections for this statistical study were taken in white noise form with $\boldsymbol{\sigma} = 1$. This was done so as not to specialize to any particular variation of Fourier coefficients with mode number n. Although use of the $n^{-1/2}$ variation suggested in this paper looks promising, other forms may be proposed in the future based on knowledge or measurements of imperfections for particular manufacturing methods. The comparisons in Figs. 6 and 7 show that the statistics will be similar for a range of amplitude variations with n.

The statistics of peak-to-peak amplitudes were obtained by calculating both negative-to-positive and positive-to-negative amplitude differences for all the peaks in the 16 buckle shapes. A histogram of the resulting values is given in Fig. 8. The histogram is sufficiently filled in that it is taken to represent the distribution of the universe of buckle shapes. It has a fairly well-defined maximum probability near 140 units of magnitude and a finite probability at zero magnitude, reflecting the many small wiggles seen in the buckle shapes. The average amplitude is 152 units and the standard deviation is 83 units.

Estimates of Buckle Wave Population Statistics

The isolated vertical tic marks labeled 152 and ± 83 on either side at the top of Fig. 8 are drawn at the average amplitude and at one standard deviation above

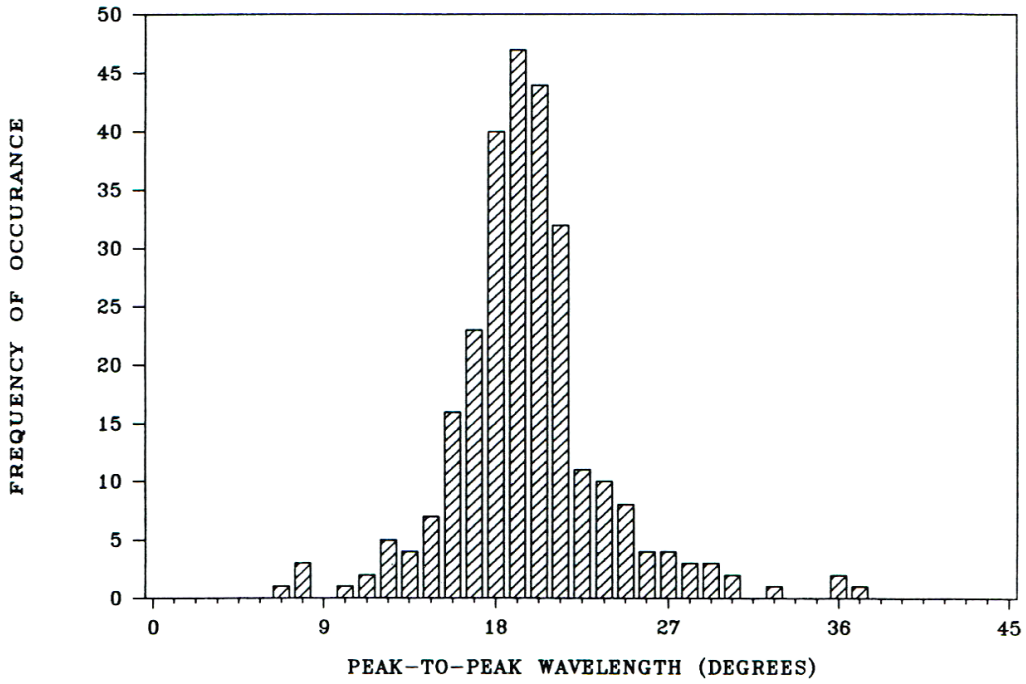

Figure 9: Histogram of buckle wavelengths for same set of results as in Fig. 8.

and below the average. The bars drawn just below the 152 and +83 tic marks give the range of average values and standard deviations calculated for the individual buckle shapes. These demonstrate that statistics calculated from buckle waves in a single buckling calculation give reasonably good estimates for the statistics of the universe of buckle waves. Thus, in finite element analyses, it appears that one or two calculations should give good estimates for buckle statistics.

Fig. 9 gives the distribution of wavelengths for the collection of 16 buckle shapes. The distribution has a pronounced maximum near 19 degrees. Nearly all the wavelengths lie between 10 and 30 degrees. An explicit formula for the mean wavelength as a function of time is given in Lindberg & Florence 1987.

CONCLUSIONS

We have shown that Fourier series with random coefficients having a Gaussian distribution with zero mean value and standard deviation $\boldsymbol{\sigma}$ give an imperfection representation that leads to buckle forms similar to those observed in experiments. For use in finite element analysis, the initial shape of the structure can be specified as the sum of this series to an upper mode number limit N, found from existing analytical results for similar structural parameters. A conservative distribution of imperfection coefficients, which relaxes the accuracy required in specifying N and the corresponding size of the finite elements while assuring participation of higher modes, results by taking $\boldsymbol{\sigma} = Chn^{-1/2}$ for cylindrical shells under radial impulse.

The number of buckles in typical calculations is large enough that the statistics of the universe of buckle waves for the problem at hand can be estimated to reasonable accuracy by the statistics of the waves in one or two calculations.

The amplitude coefficient C can be found from experimental results interpreted by closed-form theory [Eq. (41)], increased by about a factor of 3 to account for neglect in the closed-form theory of thrust reduction from buckling deformation. Similar random imperfection forms for more general loading and structures may also prove useful.

ACKNOWLEDGEMENT

This work was supported by Defense Nuclear Agency under Contract DNA 001-83-C-0139, RDT&E RMSS Codes B3420 83466 N99QAXAK 00039 H259OD and B3420 84464 N99QMXAK 00019 H2590D.

APPENDIX I.—REFERENCES

Abrahamson, G. R., and Goodier, J. N. "Dynamic Plastic Flow Buckling of a Cylindrical Shell from Uniform Radial Impulse," *Proc. U.S. Natl. Congress of Appl. Mech.*, Berkeley, CA, pp. 939-950, June 1962.

Lilly, W. E. "The Strength of Columns," *Trans. ASCE*, **76**, pp. 258-274, 1913.

Lindberg, H. E., and Anderson, D. L. "Dynamic Pulse Buckling of Cylindrical Shells Under Transient Lateral Pressures," *AIAA J.*, **6**, 4, pp. 589-598, April 1968.

Lindberg, H. E., and Florence, A. L. *Dynamic Pulse Buckling*, Martinus Nijhoff Publishers, Dordrecht, The Netherlands, Kluwer Academic Publishers, U.S. and Canada distributor, Hingham, MA, 1987.

Marston, A. "Correspondence on the Theory of the Ideal Column," *Trans. ASCE*, **39**, pp. 108-120, 1898.

Rice, S. O. "Mathematical Analysis of Random Noise," in *Selected Papers on Noise and Stochastic Processes*, Nelson Wax, ed., Dover Publications, New York, NY, 1954, pp. 133-294.

Salmon, E. H. "Columns," London, 1921, data reproduced by S. P. Timoshenko and J. M. Gere in *Theory of Elastic Stability*, 2nd ed., McGraw-Hill Book Co., New York, 1961.

APPENDIX II.—NOTATION

The symbols on the following page are used in this paper:

A, B, C = constants
E_t = material tangent modulus
G = amplification function
K = material stress-strain shape parameter
L = length of Euler column
M = sample size of uniform random numbers
N = number of summed modes
R = integral function, Eq. (22)
R_1 = integral function, Eq. (38)
a = (with no subscript) shell radius
a = coefficients of cosine displacement terms
b = coefficients of sine displacement terms
c = distance from neutral axis to extreme fiber
c_p = plastic wave speed, Eq. (13)
h = shell wall thickness
n = mode number
p = argument parameter, Eq. (20)
r = radius of gyration of column section
s = wave number parameter, Eq. (13)
t = time
u = dimensionless displacement
w = radial deformation, positive inward
x = uniformly distributed random variable
y = Gaussian-distributed random variable
z = Gaussian-distributed random variable with zero mean value
α = (with no subscript) shell thickness parameter
α = coefficients of cosine imperfection terms
β = coefficients of sine imperfection terms
δ = coefficient of single-mode imperfection
η = wave number
θ = angular coordinate
ρ = material density
σ_y = yield stress
$\boldsymbol{\sigma}$ = standard deviation of α_n and β_n
τ = dimensionless time, Eq. (20)
$\hat{\tau}$ = dimensionless time, Eq. (13)

Subscripts

i = initial imperfection
max = maximum value of function
n = mode number index

Operators

$d(\ )$ = differential
$(\ )'$ = differentiation with respect to θ
$\dot{(\ )}$ = differentiation with respect to τ
$\overline{(\ )}$ = average value